Published in final edited form as:
Nat Cell Biol. 2013 June ; 15(6): 677–687. doi:10.1038/ncb2743.

The Collagen Receptor Discoidin Domain Receptor 2 Stabilizes Snail1 Protein to Facilitate Breast Cancer Metastasis

Kun Zhang[1,3], **Callie A. Corsa**[1,2,3], **Suzanne M. Ponik**[4], **Julie L. Prior**[1,5], **David Piwnica-Worms**[1,3,5], **Kevin W. Eliceiri**[6], **Patricia J. Keely**[4,6], and **Gregory D. Longmore**[1,2,3,7]

[1]BRIGHT Institute, Washington University, St. Louis, MO, 63110

[2]Department of Medicine, Washington University, St. Louis, MO, 63110

[3]Department of Cell Biology and Physiology, Washington University, St. Louis, MO, 63110

[4]Department of Cell and Regenerative Biology, University of Wisconsin School of Medicine and Public Health, Madison, WI 53706

[5]Molecular Imaging Center in the Mallinckrodt Institute of Radiology, Washington University, St. Louis, MO, 63110

[6]Laboratory for Optical and Computational Imaging, University of Wisconsin School of Medicine and Public Health, Madison, WI 53706

Abstract

Increased stromal collagen deposition in human breast tumours correlates with metastases. We show that activation of the collagen I receptor DDR2 regulates Snail1 protein stability by stimulating ERK2 activity, in a Src-dependent manner. Activated ERK2 directly phosphorylates Snail1, leading to Snail1 nuclear accumulation, reduced ubiquitination, and increased protein half-life. DDR2-mediated stabilization of Snail1 promotes breast cancer cell invasion and migration in vitro, and metastasis in vivo. DDR2 expression was observed in the majority of human invasive ductal breast carcinomas studied, and was associated with nuclear Snail1 and absence of E-cadherin expression. We propose that DDR2 maintains Snail1 protein level and activity in tumor cells that have undergone EMT, thereby facilitating continued tumor cell invasion through collagen I-rich ECM by sustaining the EMT phenotype. As such, DDR2 could be an RTK target for the treatment of breast cancer metastasis.

Keywords

Discoidin Domain Receptor (DDR); Snail; Epithelial Mesenchymal Transition (EMT); Collagen

[7] Corresponding author, Greg Longmore, Departments of Medicine and Cell Biology and Physiology, The BRIGHT Institute, Washington University School of Medicine, Campus Box 8220, Rm. 770 McDonnell Sciences Building, 660 South Euclid Avenue, St. Louis, MO 63110, glongmor@dom.wustl.edu Phone: 1-314-362-8834.

Author Contribution

K.Z, C.A.C, S.M.P, and J.L.P were involved in project planning, experimental work and data analysis. D.P-W, K.W.E, P.J.K, and G.D.L were involved in project planning and data analysis. G.D.L. wrote the manuscript. D.P-W and P.J.K provided editorial assistance in the writing of the manuscript.

Conflict of Interests Statement

The authors declare that there are no competing commercial interests in relation to the submitted work.

INTRODUCTION

Tumor-microenvironment interactions are critical for tumor development and metastasis. In addition to alterations in cell types and their function, the stroma associated with primary tumours also exhibits increased deposition of matrix proteins, including fibrillar collagens. In human breast tumors and transgenic mouse models increased collagen in the tumor stroma correlates with metastases[1, 2], and can increase stromal stiffness or tension, influencing breast tumor invasion through tumor cell integrin-dependent mechanotransduction signaling[3]. Breast tumor cells also preferentially migrate along linear collagen fibrils near the tumor-extracellular matrix (ECM) boundary[4]. Although integrins are important collagen receptors for tumor cell invasion and migration, the role of other collagen receptors, such as the discoidin domain receptors (DDR), in cancer development and metastasis has not been extensively explored[5].

DDRs are distinctive receptor tyrosine kinases (RTKs) in that their ligands are fibrillar collagens, their activation kinetics is slow, and they may exist as preformed dimers in the absence of ligand[6]. DDR1 is present in epithelial but not mesenchymal cells, whereas DDR2 is expressed in mesenchymal cells and not epithelia. DDR2 displays more selective ligand specificity and is activated by collagens I and III, that are abundant in the ECM. DDR1 has broader collagen specificity that includes collagen IV, a major component of the basement membrane (BM).

Epithelial-mesenchymal transitions (EMT) contribute to breast cancer metastasis[7]. EMT facilitates primary tumor invasion through the BM and migration through the tumor associated stroma or ECM by suppressing tumor cell-cell adhesion and stimulating tumor cell invasion and migration [8]. Various signals generated within the tumor microenvironment activate tumor cell intrinsic transcription factors considered to be inducers of EMT, such as Snail1, Snail2 (Slug), Twist1 and ZEB[9–11].

Human and mouse cancer cell line experiments and human pathology studies implicate Snail1 in breast cancer metastasis[9, 12, 13]. Snail1 protein, which has a very short half-life is degraded by the proteasome, is predominantly present in tumor cells at the tumor-ECM boundary and in mesenchymal cells within the tumor associated stroma[13], whereas Snail1 mRNA is more broadly expressed throughout the primary tumor. Although EMT stimulating signals (e.g., TGFβ) induce Snail1 transcription, post-transcriptional and post-translational regulation influence Snail1 protein stability and subcellular localization, which is critical for Snail1's capacity to induce or sustain cancer EMT[14–16]. Given the distinct pattern of Snail1 mRNA and protein levels in tumors, the environmental signals regulating Snail1 protein stability likely originate at the tumor-ECM boundary. The identity, mechanism of Snail1 protein stabilization, and functional consequences of these signals on metastasis are only beginning to be determined[15, 16].

Here we show that the collagen receptor DDR2 stabilizes the Snail1 protein and is critical for breast cancer invasion and migration in vitro and for metastasis in vivo. We propose that DDR2 contributes to breast cancer metastasis by sustaining Snail1 protein stability and activity in tumor cells that have undergone EMT, to promote their invasion and migration through collagen I-enriched tumor-associated matrix.

RESULTS

DDR2 stabilizes cellular Snail1 protein level, post-transcriptionally

We previously identified DDR2 in a human kinome/phosphatome siRNA screen for regulators of total cellular Snail1 protein level[16]. RNAi-mediated depletion of DDR2, but

not DDR1, in HEK293 cells that stably expressed a bioluminescent Snail1 fusion protein, Snail1-Clic Beetle Green (Snail1-CBG)[16], reduced Snail1-CBG bioluminescence and protein level without affecting transcription of Snail1 or Snail1-CBG (Supplementary Fig. 1a,b).

DDR2 depletion in human MDA-MB-231 and mouse 4T1 cells that have undergone EMT resulted in decreased Snail1 protein without affecting Snail1 transcription (Fig. 1a,b), demonstrating that DDR2 also affected endogenous Snail1 levels. DDR2 depletion also affected other EMT inducers: Snail2 protein was slightly diminished, ZEB1 level increased slightly, whereas Twist1 was unchanged (Fig. 1a). Depletion of DDR2 or Snail1 in MDA-MB-231 cells that stably expressed bioluminescent Snail1-CBG, reduced Snail1-CBG bioluminescence, Snail1-CBG protein and endogenous Snail1 protein levels (Figs. 1c,d). Thus, Snail1-CBG bioluminescence could serve as an approximation of cellular Snail1 protein level to allow live cell analyses.

Overexpression of DDR2 in MDA-MB-231 or 4T1 cells increased Snail1 protein (Fig. 1e,f) without affecting mRNA levels (Supplementary Fig. S1c). This depended on DDR2 kinase activity, as overexpression of a “kinase-dead” DDR2 form did not affect Snail1 protein level (Fig. 1e). Overexpression of DDR1 may slightly increase Snail1 levels (Fig. 1f). These experiments indicated that DDR2 stabilized Snail1 protein without affecting Snail1 transcription.

Collagen I-induced stabilization of Snail1 protein requires DDR2 and can occur independently of integrin or TGFβR

Addition of HEK293 cells, co-transfected with myc-DDR2 and Snail1-Flag, or MDA-MB-231 cells to collagen I resulted in tyrosine phosphorylation and activation of DDR2 and increased Snail1 protein level (Fig. 2a, b), in contrast to exposure of MDA-MB-231 cells to collagen IV, fibronectin, or gelatin which had little effect on Snail1 levels (Fig. 2b). DDR2 depletion in MDA-MB-231 cells abrogated the increase in Snail1 protein following collagen I stimulation (Fig. 2b). Snail1 protein was stabilized by exposing MDA-MB-231 cells to collagen I in a two-dimensional or three-dimensional context (Supplementary Fig. S1d), and this was also the case for MDA-MB-231 cells containing Snail1-CBG, which led to increased Snail1-CBG bioluminescence and protein level (Supplemental Fig. S1e, f).

When MDA-MB-231 cells were mixed with neutralizing antibodies against β1-integrin, prior to and during their exposure to collagen I, Snail1 cellular protein level increased despite inhibition of integrin signaling (e.g., pFAK) (Fig. 2c). Inhibition of TGFβ signaling in MDA-MB-231 cells also had no effect (Fig. 2d), despite TGFβ increasing Snail1-CBG protein level in the absence of collagen I stimulation (Supplemental Fig. S1g), indicating that collagen I-induced stabilization of Snail1 protein level required DDR2 and could occur independently of integrin and TGFβ.

DDR2 expression is induced during EMT but is not required for EMT induction

Normal breast epithelial cells (MCF-10A) do not express Snail1[12]. When exposed to TGFβ they undergo EMT and Snail1 expression is induced, DDR2 protein expression increased, and DDR1 protein expression decreased (Fig. 2e). DDR2 was not required for TGFβ–dependent EMT induction in MCF-10A cells, as DDR2 depletion minimally affected EMT (Fig. 2e). Consistent with a role for DDR2 in stabilizing Snail1 protein, Snail1 protein levels were reduced in DDR2-depleted cells as compared to control cells following EMT (Fig. 2e). Constitutive overexpression of Snail1 in MCF-10A cells induces TGFβ-independent EMT (Fig. 2f)[12], however, DDR2 overexpression did not induce morphological or biochemical

EMT (Fig. 2f). These results indicated that although DDR2 expression was induced during EMT, the presence or absence of DDR2 did not influence TGFβ-induced EMT.

DDR2 influences breast cancer cell invasion and migration ex vivo and metastases in vivo

A major function for Snail1 during cancer metastasis is induction of invasion through the BM and migration through the ECM[8]. Depletion of Snail1 and DDR2 in 4T1 and MDA-MB-231 cells inhibited their migration in 3D collagen I matrices (Fig. 3a and Supplementary Fig. S2a), without influencing their proliferation (Fig. 3b and Supplementary Fig. S2b) and also inhibited cell invasion through matrigel (Supplementary Fig. S3c).

To determine whether DDR2 influenced breast cancer cell metastases in vivo Snail1 or DDR2 were stably depleted in 4T1-Luc/GFP cells and equal numbers of cells were surgically implanted into the breast tissue of syngeneic Balb/cJ mice. After correcting for the small differences observed in the growth of the Snail1- and DDR2-depleted primary tumors in vivo (Fig. 3c, d), reduced lung metastases were observed in DDR2- and Snail1-depleted tumor-bearing mice (Fig. 3e–g). Both the number of mice that developed lung metastases (Fig. 3f) and the extent of metastasis present (Fig. 3g) were reduced in mice injected with DDR2-depleted tumor cells. Fluorescent GFP imaging of isolated lungs (Supplementary Fig. S2d) and histologic analysis of lung slices (Supplementary Fig. S2e) confirmed the bioluminescent results, demonstrating that DDR2 promoted breast to lung metastases in vivo.

Collagen I activated DDR2 induces collagen I transcription and remodeling of collagen fibers at the tumor-ECM boundary

During breast cancer progression, increased deposition of ECM proteins, particularly collagens, can occur within and near the primary tumor[17, 18]. This is associated with poor outcome due to increased local invasion and distant metastasis[19, 20]. The collagen fibers deposited near tumours can also thicken and realign, and tumors with fibers aligned perpendicularly to the tumor edge have an increased propensity to invade and metastasize. This observation has led to a classification of “Tumor Associated Collagen Signatures” or TACS in primary breast tumors that correlates with breast tumor progression and patient outcome[2, 4, 21]. The DDRs have been implicated in both collagen synthesis by cells and remodeling of the ECM[22–24].

Collagen fiber alignment was measured and TACS was calculated using second harmonic generation imaging of collagen fibers at the tumor/ECM boundary. Tumors depleted of Snail1 or DDR2 showed an increase in TACS-2, the non-invasive collagen signature, and decrease in TACS-3, the invasive collagen signature, compared to control tumors (Fig. 4a, b; Supplementary Fig. S3a, b), suggesting that breast cancer cell-expressed DDR2 might influence collagen remodeling by invasive tumors.

Addition of MDA-MB-231 cells to collagen I coated plates, induced collagen I mRNA transcription by 2–2.5 fold, and depletion of DDR2 or Snail1 reduced this transcriptional response (Fig. 4c). Similar results were observed with 4T1 cells (Supplementary Fig. S3c). Despite this effect upon collagen I transcription there was no discernable change in the collagen content of DDR2-depleted 4T1 tumors compared to control tumors, as determined from trichrome staining (Supplementary Fig. S4a).

DDR2 activated ERK2 associates with and phosphorylates Snail1

Stabilization of Snail1 protein by collagen I-induced DDR2 activation was unlikely to be the result of direct phosphorylation by DDR2, as tyrosine phosphorylation of Snail1 has not been observed in phosphoproteomic analyses[16, 25].

Addition of MDA-MB-231 cells to collagen I led to activation of ERK1/2, but not p38, JNK or Akt, which was shown by pharmacological inhibitor studies to be required for stabilization of Snail1 protein (Fig. 5a), but had no effect on Snail1 mRNA levels (Supplementary Fig. S5a). RNAi-depletion revealed that ERK2, but not ERK1, was required for Snail1 protein stabilization following collagen I activation (Supplementary Fig. S5b). ERK2 was recently shown to be critical for EMT induction of RasV12-transfected MCF-10A cells[26]. Sequence analysis of Snail1 revealed the presence of potential D-domain and DEF-domain ERK docking sites (Fig. 5b)[27]. In MDA-MB-231 cells a small amount of endogenous ERK2 associated with endogenous Snail1, and this association increased when cells were added to collagen I, yet blocked by pretreating cells with the MEKK inhibitor PD98059 (Fig. 5b). Snail1 and ERK2 readily co-immunoprecipitated from HEK293 cells co-transfected with both (Supplemental Figs. S5c, d and S6a). Mapping experiments indicated that the Snail1 D-domain docking site, but not the DEF-domain, was important for ERK2 association (Supplementary Fig. S5c). Mutation of the D-domain ERK docking site in Snail1 (RK-MM) reduced its association with ERK2 (Supplementary Fig. S5d). Mutation of the D-domain recognition region of ERK2 (D319N), but not the DEF-domain recognition region (Y261A)[26] reduced ERK2-Snail1 association (Supplemental Fig. S6a). In vitro kinase assays with purified ERK2 and purified GST-Snail1 proteins containing S-A mutations in three potential ERK phosphorylation sites identified, revealed that S82 and S104 were phosphorylated (Fig. 5c).

To determine if phosphorylation of Snail1 by ERK2 was functionally relevant we tested whether mutation of S82 and S104 affected Snail1 protein stability in response to collagen I. When expressed in MDA-MB-231 cells, the protein half-life of an 82/104A Snail1-CBG mutant was half that of WT Snail1 (Fig. 5d). When cells were added to collagen I, WT Snail1-CBG half-life increased whereas the half-life of 82/104A Snail1-CBG remained unaltered (Fig. 5d). In contrast to WT Snail1-CBG-expressing cells, which required DDR2 for Snail1 stabilization in response to collagen I, the stability of 82/104A Snail1-CBG in collagen I stimulated cells was unaffected by the presence or absence of DDR2 (Supplemental Fig. S6b).

Depletion of endogenous Snail1 in MDA-MB-231 cells and concurrent rescue with RNAi-resistant WT Snail1, using dual copy lentiviruses[28], completely restored 3D cell migration to Snail1-depleted cells, whereas rescue with the 82/104A mutant (2A) or ERK D domain mutant of Snail1 (RK-MM) only partially rescued the migration defect of Snail1 depleted cells (Fig. 5e; Supplemental Fig. S7a). Control Western blots indicated that endogenous Snail1 was effectively depleted and that RNAi-resistant rescue mutants were expressed at levels equivalent to endogenous Snail1 (Supplementary Fig. S7b). Endogenous DDR2 was not affected by these manipulations (Supplementary Fig. S7b).

Both WT Snail1-CBG and 82/104A.Snail1-CBG were stabilized by proteasome inhibition, but only WT Snail1-CBG protein was stabilized by exposure to collagen I (Fig. 6a). Snail1 protein is degraded by proteasomes in the cytosol and when nuclear is more stable[14, 16]. When transfected in MCF-10A cells, WT Snail1 was predominantly nuclear whereas 82/104A Snail1 was predominantly cytosolic (Fig. 6b), however, Leptomycin B treatment, to inhibit nuclear export, resulted in accumulation of both forms in the nucleus (Fig. 6b). This suggested that the 82/104A mutant was not retained in the nucleus and that ERK2-mediated phosphorylation of Snail1 leads to its nuclear accumulation and protection from ubiquitination and subsequent proteosomal degradation. When MDA-MB-231 cells were treated with collagen I, the increase in WT Snail1 protein was exclusively nuclear (Fig. 6c). In HEK293 cells transfected with DDR2, Snail1, and HA-tagged ubiquitin and then stimulated with collagen I, in the absence of proteosommal inhibition, immunoprecipitated 82/104A Snail1 was more ubiquitinated than WT Snail1 (Fig. 6d). These results indicated

that phosphorylation of Snail1 on 82S and 104S by Collagen I-DDR2-stimulated ERK2 led to its accumulation in the nucleus and decreased ubiquitination. Thus Snail1 protein was stabilized, its level increased, and Snail1's capacity to mediate tumor cell invasion and migration was maintained.

Delineation of the intracellular signaling pathway whereby DDR2 leads to Snail1 protein stabilization and tumor cell invasion/migration

To evaluate the contribution of more proximal DDR2-activated signaling enzymes to ERK2 activation and Snail1 stabilization we asked whether FAK or Src was required for collagen I induced Snail1 protein stabilization[5, 29]. FAK depletion in MDA-MB-231 cells did not affect ERK activation or Snail1 stabilization (Supplementary Fig. S8a). Src, however, was required for collagen I induced stabilization of Snail1 (Supplemental Fig. S8b).

Glycogen Synthase kinase 3β (GSK3β) is a well-established regulator of Snail1 protein stability[14]. ERK can associate with and inactivate GSK3β by acting as a scaffold for p90RSK and GSK3β[30], and this ERK-p90RSK-GSK3β pathway can be stimulated by RTKs such as HER2[30, 31]. Thus, we tested whether DDR2 activation could modulate GSK3β activity downstream of ERK2. pS9-GSK3β (inhibited) was present in unstimulated MDA-MB-231 cells, and its levels were increased when cells were added to collagen I (Fig. 7a). DDR2 depletion in unstimulated cells decreased the level of inhibited GSK3β, however when these cells were added to collagen I the level of pS9-GSK3β increased to the same extent as in control cells (Fig. 7a). This suggested that when breast cancer cells interacted with collagen I, GSK3β activity was inhibited independently of DDR2. This DDR2-independent pathway could also contribute to stabilization of Snail1 protein in response to collagen. We tested this possibility by assessing whether depleting GSK3β affected Snail1 stabilization following exposure to collagen I. Snail1 protein increased 2.5–3.5 fold in unstimulated cells indicating that GSK3β contributed to basal Snail1 levels (Fig. 7b). However, when GSK3β-depleted cells were added to collagen I Snail1 protein increased to the maximal level seen in control cells (Fig. 7b), indicating that although GSK3β contributed to Snail1 protein stabilization, it did so in unstimulated cells and was not necessary for collagen I-induced stabilization of Snail1.

To determine if ERK2 activation in response to collagen I was required for GSK3β inhibition and Snail1 stabilization, ERK2 was depleted in MDA-MB-231 cells. In unstimulated cells, depletion of ERK2 resulted in decreased inhibition of GSK3β (Fig. 7c); however, when these cells were added to collagen I, pS9-GSK3β levels were equal to those in control or ERK1-depleted cells (Fig. 7c). As expected, depletion of ERK2 resulted in decreased level of Snail1 protein in unstimulated cells (Fig. 7c), which was equivalent to Snail1 levels in DDR2-depleted cells (Fig. 7a). Therefore, ERK2 was required to inhibit GSK3β in unstimulated cells. When ERK2-depleted cells were added to collagen I, Snail1 protein levels increased to 2-fold, whereas those in control cells increased 3-fold (Fig. 7c). The level of Snail1 protein in ERK2 depleted cells stimulated with collagen I did not approach that observed in control or ERK1-depleted cells, despite equivalent levels of pS9-GSK3β (Fig. 7c). Taken together, these results indicated that although ERK2 also stabilized Snail1 by inhibiting GSK3β, this was a minor contribution.

These signaling experiments suggested a pathway whereby Collagen I mediated activation of DDR2 stabilized Snail1 protein (Fig. 7d). Collagen I activated DDR2 stimulated ERK2 activity, in a Src-dependent manner. ERK2 then interacted with and phosphorylated Snail1 on S82 and S104 and inhibited GSK3β activity, with both effects contributing to stabilization of Snail1 protein. Elevated Snail1 levels sustained both MT1-MMP production and activity[32, 33] and collagen synthesis (Fig. 4c), both of which could contribute to the remodeling of collagen fibers seen at the breast tumor/ECM interface (Fig. 4a, b).

To test this proposed pathway we depleted each component individually, and determined the activity and level of other proteins in the pathway. DDR2 depletion affected the activity or protein level of all downstream components (Fig. 7e). ERK2 depletion influenced the activity or protein level of GSK3β, Snail1, MT1-MMP, but not DDR2 (Fig. 7e). GSK3β depletion only affected the Snail1 levels in unstimulated cells and had no effect on other pathway components, or Snail1 in collagen I-stimulated cells (Fig. 7e). Snail1 depletion only affected the level of MT1-MMP (Fig. 7e). Finally, depletion of MT1-MMP did not affect Snail1 protein levels (Supplemental Fig. S8c), but was required for MDA-MB-231 cell migration in 3D collagen I gels (Supplemental Fig. S8d).

DDR2 is expressed in human invasive ductal breast cancers and correlates with nuclear Snail1, loss of E-cadherin, and increased collagen

We performed IHC on human invasive ductal (IDC) and invasive lobular breast cancer samples compared with tumor-associated normal breast tissue. Snail1 and DDR2 were not expressed in normal breast ducts or acini (Fig. 8a, b; Supplemental Fig. S8e), however, 71% of invasive ductal carcinoma cells expressed DDR2 (Fig. 8a). There was no difference in DDR2 expression and lymph node involvement (Supplemental Fig. S8e). Only 21% of invasive lobular cancers expressed low levels of DDR2 (Fig. 8a). Ongoing TCGA RNA sequence analysis of gene copy number in breast cancers[34] found that 5% of invasive breast tumors exhibited amplified copy number of the DDR2 gene and these patients had worse survival rates (Fig. 8b). 38% of IDCs were Snail1 positive and of these 91% were DDR2 positive and 81% E-cadherin negative (Fig. 8c). However, in Snail1 negative tumors 47% were DDR2 positive (Fig. 8c). Thus, DDR2 was expressed in the majority of invasive ductal breast carcinomas studied, and most of those positive for nuclear Snail1 expression also expressed DDR2 and lacked E-cadherin.

Trichrome staining was used to assess collagen content in invasive ductal carcinomas. Of IDC with increased collagen (70%), 86% were positive for DDR2, whereas 55% of collagen negative tumors (30%) were DDR2 positive (Fig. 8d). Starting with DDR2 positive tumors (77%), 78% exhibited increased collagen (Fig. 8e). But in DDR2 negative tumors (23%), 42% exhibited increased collagen (Fig. 8e). This suggested that in tumors with increased collagen content there was a strong association with the presence of DDR2, however, this was not specific as significant numbers of collagen negative tumors expressed DDR2 and a significant number of DDR2 negative tumors had increased collagen content.

DISCUSSION

We have identified the collagen receptor DDR2 as contributing to invasion, migration, and metastasis of breast cancer cells by stabilizing Snail1 protein level. Our working model posits that breast tumor environmental signals such as TGFβ or Wnt induce Snail1 transcription[14, 15] and EMT[12]. As a result tumor cells become mesenchymal and DDR2 is expressed as part of the EMT process. Following invasion through the BM tumor cells are exposed to the collagen I-rich ECM associated with breast tumors and this activates DDR2 and serves as a positive signal to maintain Snail1 protein level and activity thereby sustaining tumor cell migration leading to metastasis.

Most human invasive ductal breast cancer expressed DDR2. Although genetic events leading to DDR2 expression cannot be currently excluded, it is likely that many invasive breast cancers have undergone EMT and DDR2 expression could reflect this process. Although we observed an association between nuclear Snail1, lack of E-cadherin and the presence of DDR2, a significant proportion of Snail1 negative tumors expressed DDR2, suggesting that in addition to stabilizing Snail1, DDR2 could contribute to cancer metastasis by other means. RNA sequence analysis found that 5% of invasive breast tumors have

amplified DDR2 gene expression[34], with this single variable revealing that these patients exhibited decreased survival. Whether these tumors also express Snail1 is not known, and it would be interesting to study whether they represent the aggressive claudin-low subtype of triple negative breast cancers that exhibit mesenchymal features, including the presence of EMT inducers such as Snail1[7].

The presence of collagen fibers perpendicularly aligned to the tumor boundary predicts for increased relapse and decreased survival[4]. An increase in collagen *in vitro* drives expression of EMT markers[35], providing support for a link between increased collagen and EMT. Our studies suggest that DDR2 could provide a connection between collagen and sustained EMT. However, DDR2 is not the only collagen I receptor expressed by invasive breast cancer cells. Invasive breast cancers can exhibit increased tissue stiffness with tumor cells responding to increased ECM tension through integrin-mediated mechanotransduction[3]. Thus, integrin activity is important for breast cancer invasion[3],[36]. Whether DDR2 contributes to integrin-mediated mechanotransduction responses during tumor invasion is not known, but other RTKs have been shown to influence integrin function[37, 38]. In addition, the increase in ERK activity in tumor cells in a stiff environment was ascribed to integrin-dependent focal adhesion activation and EGFR signaling[3]. Collagen-induced DDR2 activation also led to an increase in ERK activity that contributed to Snail1 protein stabilization and tumor cell invasion/migration, raising the possibility that, in addition to integrin/FA-Rho-ROCK mediated mechanotransduction[3], Snail1 protein stabilization and EMT maintenance could also contribute to tumor cell invasion in stiff tissues. Regardless, DDR2 depletion from aggressive, metastatic breast cancer cell lines that have undergone EMT and express Snail1, led to reduced in vivo metastases, implying that DDR2, like integrin, is an important collagen receptor during breast cancer metastasis.

The collagen I-induced, DDR2-ERK2 signaling axis that maintains Snail1 protein level and activity in breast tumor cells that have undergone EMT, could contribute to the increased aggressiveness of breast cancer in women with dense breasts that are due, in part, to increased fibrillar collagen deposition[39], tumors in an involuting breast microenvironment that are associated with increased collagen deposition[40], and in breast cancer patients with extensive fibrotic reactions around the primary tumors[1]. Thus, DDR2 could be a potential target to treat breast cancer metastasis.

Supplementary Material

Refer to Web version on PubMed Central for supplementary material.

Acknowledgments

This work was supported by NIH Grants P50CA94056 to the Imaging Core of the Siteman Cancer Center at Washington University. NIH grants GM080673 and CA143868, and Susan G. Komen for the Cure KG110889 to G.D.L. C.A.C was supported by NIH grant F31CA165729

References

1. Kauppila S, Stenback F, Risteli J, Jukkola A, Risteli L. Aberrant type I and type III collagen gene expression in human breast cancer in vivo. The Journal of pathology. 1998; 186:262–268. [PubMed: 10211114]
2. Provenzano PP, et al. Collagen density promotes mammary tumor initiation and progression. BMC Med. 2008; 6:11. [PubMed: 18442412]
3. Paszek MJ, et al. Tensional homeostasis and the malignant phenotype. Cancer Cell. 2005; 8:241–254. [PubMed: 16169468]

4. Conklin MW, et al. Aligned collagen is a prognostic signature for survival in human breast carcinoma. The American journal of pathology. 2011; 178:1221–1232. [PubMed: 21356373]
5. Valiathan RR, Marco M, Leitinger B, Kleer CG, Fridman R. Discoidin domain receptor tyrosine kinases: new players in cancer progression. Cancer Metastasis Rev. 2012
6. Leitinger B. Transmembrane collagen receptors. Annu Rev Cell Dev Biol. 2011; 27:265–290. [PubMed: 21568710]
7. Perou CM. Molecular stratification of triple-negative breast cancers. The oncologist. 2010; 5(15 Suppl):39–48. [PubMed: 21138954]
8. Thiery JP, Acloque H, Huang RY, Nieto MA. Epithelial-mesenchymal transitions in development and disease. Cell. 2009; 139:871–890. [PubMed: 19945376]
9. Moody SE, et al. The transcriptional repressor Snail promotes mammary tumor recurrence. Cancer Cell. 2005; 8:197–209. [PubMed: 16169465]
10. Yang J, et al. Twist, a master regulator of morphogenesis, plays an essential role in tumor metastasis. Cell. 2004; 117:927–939. [PubMed: 15210113]
11. Drasin DJ, Robin TP, Ford HL. Breast cancer epithelial-to-mesenchymal transition: examining the functional consequences of plasticity. Breast Cancer Res. 2011; 13:226. [PubMed: 22078097]
12. Tran DD, Corsa CA, Biswas H, Aft RL, Longmore GD. Temporal and spatial cooperation of Snail1 and Twist1 during epithelial-mesenchymal transition predicts for human breast cancer recurrence. Molecular cancer research : MCR. 2011; 9:1644–1657. [PubMed: 22006115]
13. Franci C, et al. Expression of Snail protein in tumor-stroma interface. Oncogene. 2006; 25:5134–5144. [PubMed: 16568079]
14. Zhou BP, et al. Dual regulation of Snail by GSK-3beta-mediated phosphorylation in control of epithelial-mesenchymal transition. Nat Cell Biol. 2004; 6:931–940. [PubMed: 15448698]
15. Yook JI, et al. A Wnt-Axin2-GSK3beta cascade regulates Snail1 activity in breast cancer cells. Nat Cell Biol. 2006; 8:1398–1406. [PubMed: 17072303]
16. Zhang K, et al. Lats2 kinase potentiates Snail1 activity by promoting nuclear retention upon phosphorylation. The EMBO journal. 2011; 31:29–43. [PubMed: 21952048]
17. Egeblad M, Rasch MG, Weaver VM. Dynamic interplay between the collagen scaffold and tumor evolution. Current opinion in cell biology. 2010; 22:697–706. [PubMed: 20822891]
18. Schedin P, Keely PJ. Mammary gland ECM remodeling, stiffness, and mechanosignaling in normal development and tumor progression. Cold Spring Harbor perspectives in biology. 2011; 3:a003228. [PubMed: 20980442]
19. Walker RA. The complexities of breast cancer desmoplasia. Breast Cancer Res. 2001; 3:143–145. [PubMed: 11305947]
20. Kreike B, et al. Gene expression profiling and histopathological characterization of triple-negative/basal-like breast carcinomas. Breast Cancer Res. 2007; 9:R65. [PubMed: 17910759]
21. Provenzano PP, et al. Collagen reorganization at the tumor-stromal interface facilitates local invasion. BMC Med. 2006; 4:38. [PubMed: 17190588]
22. Ferri N, Carragher NO, Raines EW. Role of discoidin domain receptors 1 and 2 in human smooth muscle cell-mediated collagen remodeling: potential implications in atherosclerosis and lymphangioleiomyomatosis. The American journal of pathology. 2004; 164:1575–1585. [PubMed: 15111304]
23. Flynn LA, Blissett AR, Calomeni EP, Agarwal G. Inhibition of collagen fibrillogenesis by cells expressing soluble extracellular domains of DDR1 and DDR2. Journal of molecular biology. 2010; 395:533–543. [PubMed: 19900459]
24. Sivakumar L, Agarwal G. The influence of discoidin domain receptor 2 on the persistence length of collagen type I fibers. Biomaterials. 2010; 31:4802–4808. [PubMed: 20346496]
25. MacPherson MR, et al. Phosphorylation of serine 11 and serine 92 as new positive regulators of human Snail1 function: potential involvement of casein kinase-2 and the cAMP-activated kinase protein kinase A. Molecular biology of the cell. 2010; 21:244–253. [PubMed: 19923321]
26. Shin S, Dimitri CA, Yoon SO, Dowdle W, Blenis J. ERK2 but not ERK1 induces epithelial-to-mesenchymal transformation via DEF motif-dependent signaling events. Molecular cell. 2010; 38:114–127. [PubMed: 20385094]

27. Jacobs D, Glossip D, Xing H, Muslin AJ, Kornfeld K. Multiple docking sites on substrate proteins form a modular system that mediates recognition by ERK MAP kinase. Genes Dev. 1999; 13:163–175. [PubMed: 9925641]
28. Feng Y, et al. A multifunctional lentiviral-based gene knockdown with concurrent rescue that controls for off-target effects of RNAi. Genomics Proteomics Bioinformatics. 2010; 8:238–245. [PubMed: 21382592]
29. Ikeda K, et al. Discoidin domain receptor 2 interacts with Src and Shc following its activation by type I collagen. J Biol Chem. 2002; 277:19206–19212. [PubMed: 11884411]
30. Ding Q, et al. Erk associates with and primes GSK-3beta for its inactivation resulting in upregulation of beta-catenin. Molecular cell. 2005; 19:159–170. [PubMed: 16039586]
31. Desbois-Mouthon C, et al. Insulin and IGF-1 stimulate the beta-catenin pathway through two signalling cascades involving GSK-3beta inhibition and Ras activation. Oncogene. 2001; 20:252–259. [PubMed: 11313952]
32. Ota I, Li XY, Hu Y, Weiss SJ. Induction of a MT1-MMP and MT2-MMP-dependent basement membrane transmigration program in cancer cells by Snail1. Proc Natl Acad Sci U S A. 2009; 106:20318–20323. [PubMed: 19915148]
33. Rowe RG, et al. Mesenchymal cells reactivate Snail1 expression to drive three-dimensional invasion programs. J Cell Biol. 2009; 184:399–408. [PubMed: 19188491]
34. Cerami E, et al. The cBio Cancer Genomics Portal: An Open Platform for Exploring Multidimensional Cancer Genomics Data. Cancer Discov. 2012; 2:401–404. [PubMed: 22588877]
35. Provenzano PP, Inman DR, Eliceiri KW, Keely PJ. Matrix density-induced mechanoregulation of breast cell phenotype, signaling and gene expression through a FAK-ERK linkage. Oncogene. 2009; 28:4326–4343. [PubMed: 19826415]
36. White DE, et al. Targeted disruption of beta1-integrin in a transgenic mouse model of human breast cancer reveals an essential role in mammary tumor induction. Cancer Cell. 2004; 6:159–170. [PubMed: 15324699]
37. Mariotti A, et al. EGF-R signaling through Fyn kinase disrupts the function of integrin alpha6beta4 at hemidesmosomes: role in epithelial cell migration and carcinoma invasion. J Cell Biol. 2001; 155:447–458. [PubMed: 11684709]
38. Soung YH, Clifford JL, Chung J. Crosstalk between integrin and receptor tyrosine kinase signaling in breast carcinoma progression. BMB Rep. 2010; 43:311–318. [PubMed: 20510013]
39. Aiello EJ, Buist DS, White E, Porter PL. Association between mammographic breast density and breast cancer tumor characteristics. Cancer Epidemiol Biomarkers Prev. 2005; 14:662–668. [PubMed: 15767347]
40. McDaniel SM, et al. Remodeling of the mammary microenvironment after lactation promotes breast tumor cell metastasis. The American journal of pathology. 2006; 168:608–620. [PubMed: 16436674]

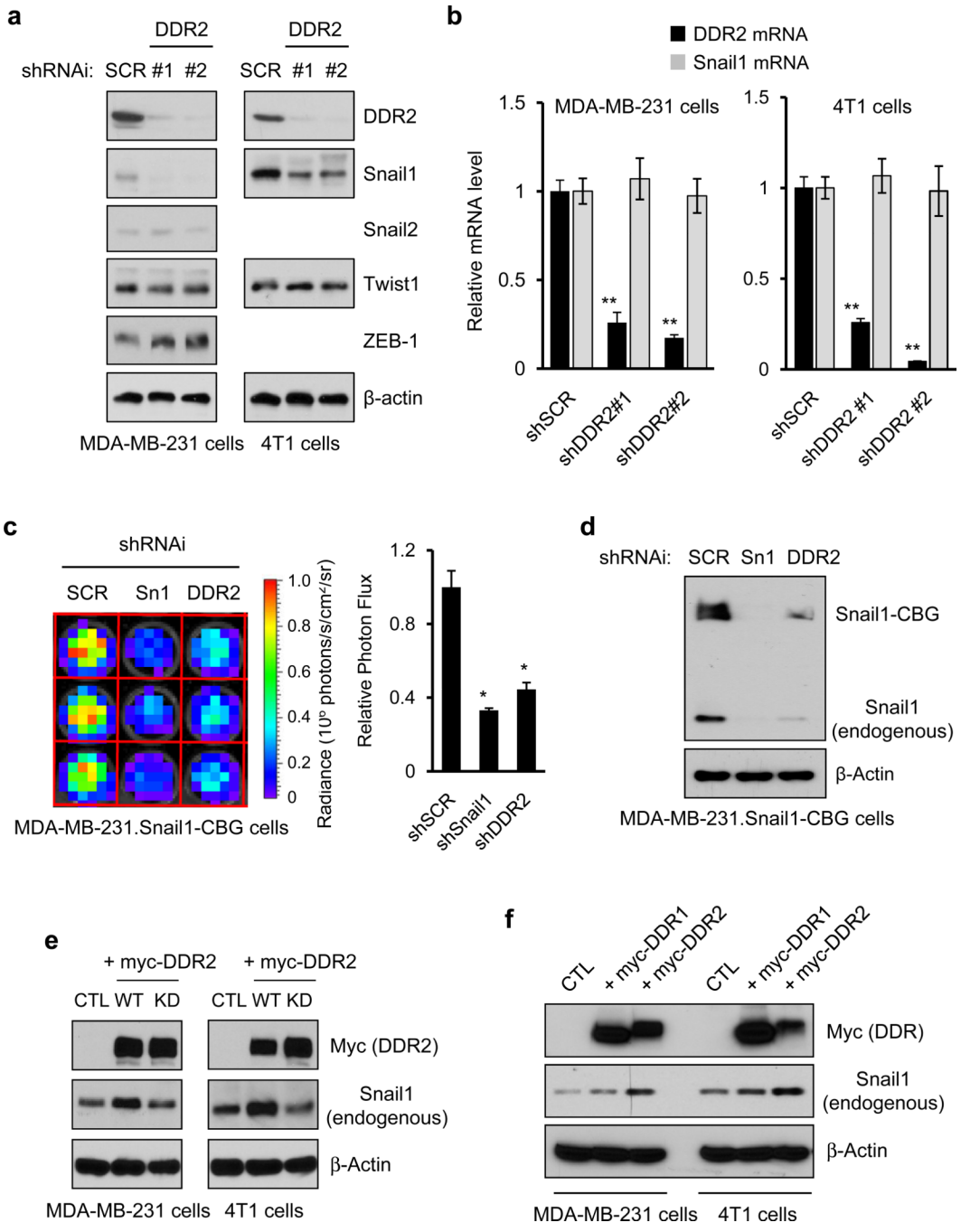

Figure 1. DDR2 stabilizes cellular Snail1 protein level, post-transcriptionally

(**a, b**) Human MDA-MB-231 or mouse 4T1 breast cancer cells were infected with lentiviruses expressing two different shRNAi targeting DDR2 (#1, #2) or control scrambled shRNAi (SCR). (**a**) Western blot was performed with the indicated antibodies. (**b**) Q-PCR determination of mRNA levels for indicated genes. Means and s.d. are shown for three independent experiments; 3 wells of cells were analyzed in each experiment. P-values were calculated using unpaired, two-sided Student's t-tests. ** P<0.01. (**c, d**) MDA-MB-231 cells containing a bioluminescent Snail1-CBG transgene were infected with lentiviruses expressing shRNAi targeting DDR2, Snail1 (Sn1), or a scrambled control (SCR). (**c**)

Bioluminescence radiance was determined and photon flux plotted relative to control cells. Means and s.d. are shown for three independent experiments; 3 wells of cells were analyzed in each experiment. P-values were calculated using unpaired, two-sided Student's t-tests. * $P<0.05$. (**d**) Western blot with indicated antibodies. (**e**) DDR2 was overexpressed in human MDA-MB-231 and mouse 4T1 breast cancer cells by infecting cells with retroviruses expressing myc-tagged wild type DDR2 (WT), myc-tagged kinase-dead DDR2 (KD), or empty vector (CTL). Western blots with the indicated antibodies were performed on cell extracts. (**f**) MDA-MB-231 or 4T1 cells were infected with retroviruses expressing myc-tagged DDR1, myc-tagged DDR2, or empty vector (CTL) and Western blots with the indicated antibodies performed on cell extracts.

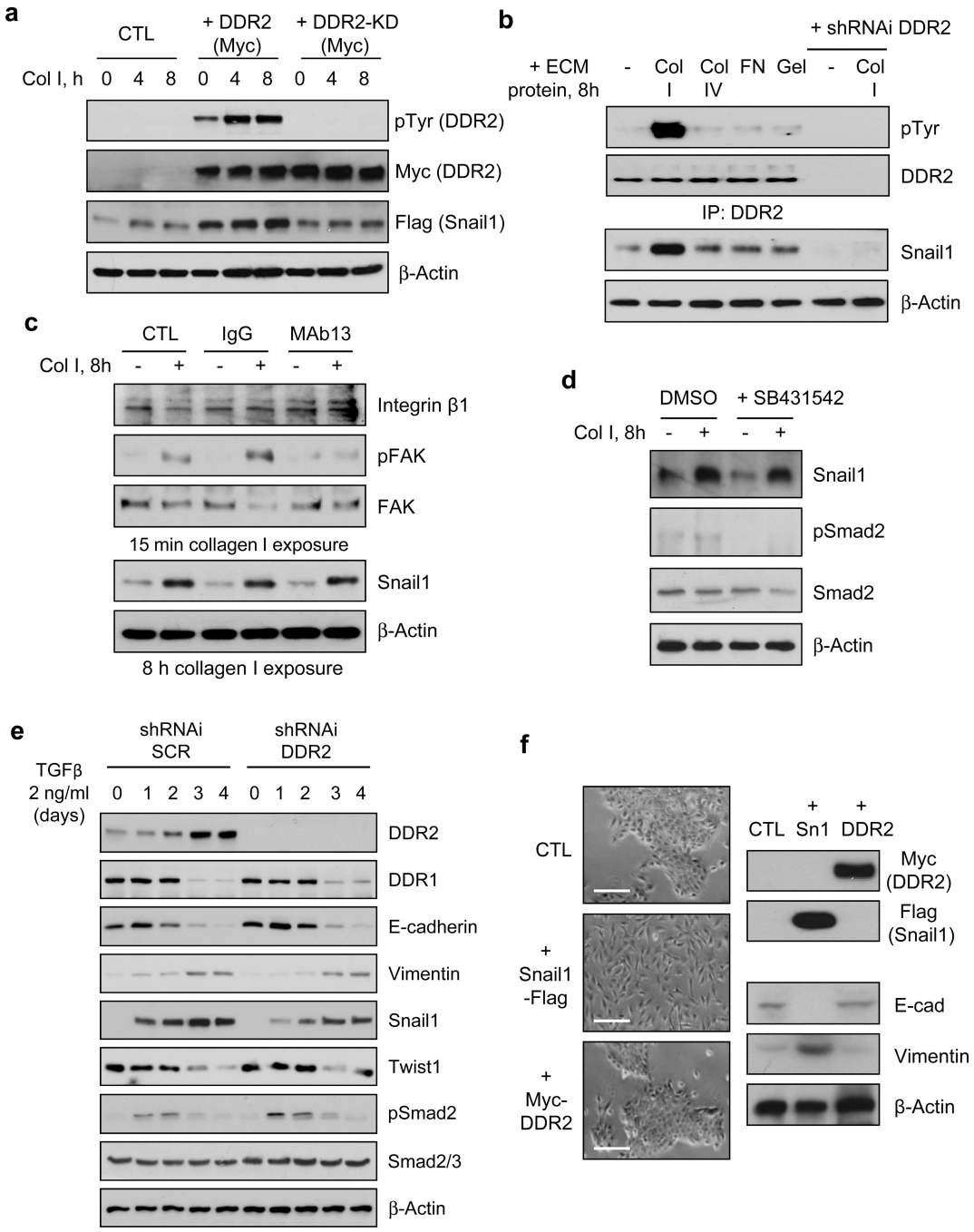

Figure 2. Collagen I-induced stabilization of Snail1 protein requires DDR2

(**a**) HEK293 cells transfected with indicated plasmids (CTL – empty vector) were added to plates coated with collagen I (2 mg/ml) for indicated times (hours). Western blots were performed. (**b**) Human MDA-MB-231 cells were added to plates coated with ECM proteins for 8 hours: FN – fibronectin; Gel – gelatin. DDR2 was immunoprecipitated and bound products Western blotted with pTyr or DDR2 antibodies (upper panels). Western blots of cell extracts (lower panels). In the last two lanes cells were depleted of DDR2 with shRNAi. (**c**) MDA-MB-231 cells were untreated (CTL), pretreated with mouse IgG or neutralizing antibody against β1-integrin (MAb13) for 2 hours, added to collagen I coated (+) or

uncoated plates (−) for 15 minutes or 8 hours. Western blots were performed. (**d**) MDA-MB-231 cells were treated with DMSO or SB431542 (10 μM), an inhibitor of TGFβ signaling, before addition to plates coated with collagen I (+) or uncoated (−) for 8 hours. Western blots were performed. (**e**) MCF-10A cells infected with DDR2 or scrambled control (SCR) shRNAi lentiviruses were treated with TGFβ (2 ng/ml) continuously for 4 days to induce EMT. Western blots were performed on cell extracts each day for 4 days of TGFβ treatment. (**f**) MCF-10A cells were infected with empty (CTL), Snail1-Flag, or myc-DDR2 retroviruses and cultured without TGFβ for 4 days. Phase images of cells on day 4 (left). Scale bar 100 μm. Western blots of day 4 cell extracts with the indicated antibodies (right).

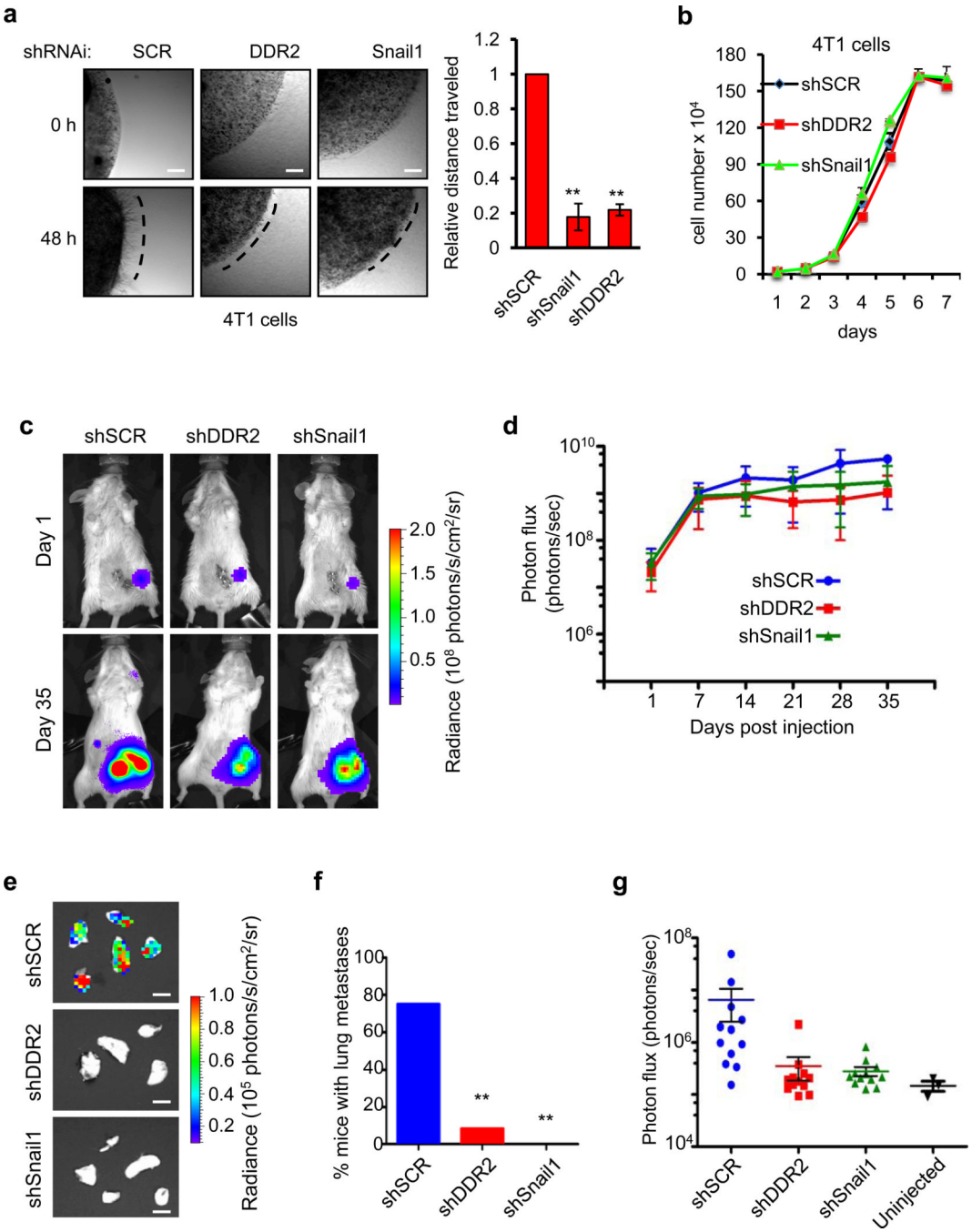

Figure 3. DDR2 influences breast cancer cell migration in vitro and metastases in vivo

(**a**) Cell migration in 3D collagen gels of 4T1 cells depleted of Snail1, DDR2, or control (SCR). Distance traveled relative to control cells was determined at 48 h. Scale bar 250 μm. Means and s.d. for five experiments; ten cell aggregates analyzed each experiment. P-values calculated using unpaired, two-sided Student's t-tests. ** P<0.01. (**b**) 4T1 cell proliferation curve: control (black line), DDR2-depleted (red line), or Snail1-depleted cells (green line). Means and s.d. for five experiments; three wells of cells analyzed each experiment. (**c**) Representative images of BALB/cJ mice whose breast tissue was implanted with 1×10^6 4T1-Luc/GFP control (shSCR), DDR2 depleted (shDDR2), or Snail1 depleted (shSnail1)

cells. Whole mouse bioluminescence performed day 1 and 35 post-implantation. (**d**) Growth curve of primary tumors, as determined by bioluminescence. Means and s.d.; data derived from one experiment of twelve mice per condition. (**e**) Bioluminescence of representative images of lungs 5 weeks post tumor cell implantation into breast. Scale bar 0.5 cm. (**f**) Percent of mice with lung metastases 5 weeks post-injection, as determined by lung bioluminescence. Means and s.d.; data derived from one experiment of twelve mice per condition. P-values calculated using 2-tailed Fisher Exact test. ** $P < 0.01$. (**g**) Total bioluminescence of lungs imaged 5 weeks post tumor implantation. Means and S.E.M.; data derived from one experiment of twelve mice per condition. Uninjected control mice n=3. Primary data for (**d**) and (**g**) are provided in the Statistics Source Data file in the supplementary information.

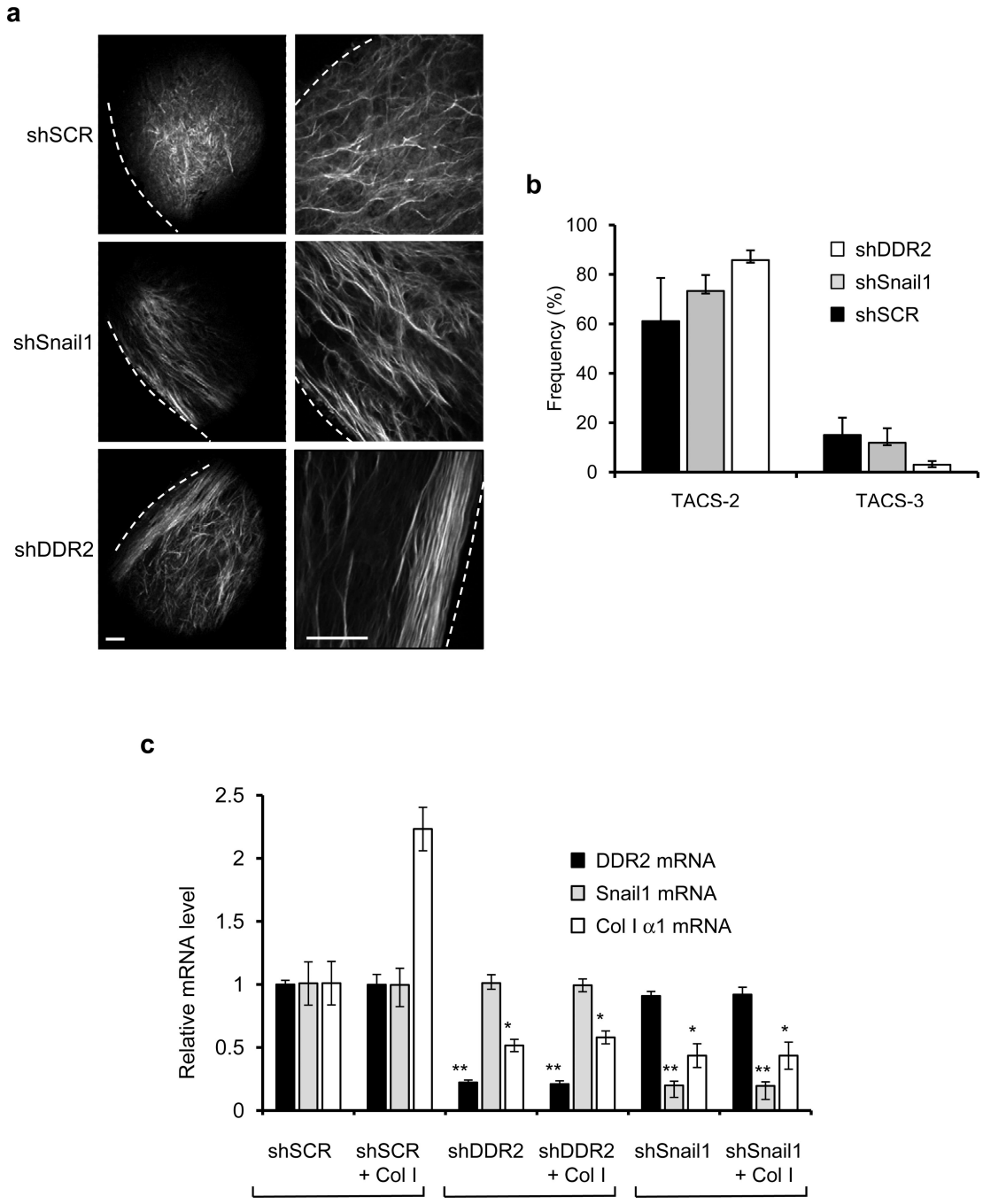

Figure 4. Collagen fiber alignment at tumor-ECM boundary

(**a**) Second harmonic generation imaging of collagen fibers at the tumor-ECM boundary of primary tumors from xenografts of 4T1 cells transduced with control shSCR, shSnail1, or shDDR2 RNAi expressing lentiviruses. Dashed line represents the tumor boundary. Scale bars = 100μm. Both magnifications are of the same tumor but at different locations. (**b**) Using CurvAlign software, the angle of collagen fibers relative to the tumor boundary was determined. Each column consists of n=3 tumors with three fields of view for each (nine images for each tumor). All angles from 0–30 degrees were catagorized as “TACS-2”, parallel to the tumor boundary. Fibers in the range of 60–90 degrees were categorized as

"TACS-3", perpendicular to the tumor boundary. Means and S.E.M. are shown for one experiment. Primary data are provided in the Statistics Source Data file in the supplementary information. (**c**) MDA-MB-231 cells shRNAi-depleted of Snail1 (shSnail1), DDR2 (shDDR2), or control (SCR) were added to uncoated plates or plates coated with 2 mg/ml of collagen I for 8 hours and Q-PCR determination of mRNA levels for collagen I (black columns), Snail1 (light gray columns), and DDR2 (dark gray columns) relative to control cells not added to collagen-coated plates was determined. Means and s.d. for three independent experiments; three wells of cells were analyzed each experiment. P-values calculated using unpaired, two-sided Student's t-tests. * $P<0.05$; ** $P<0.01$.

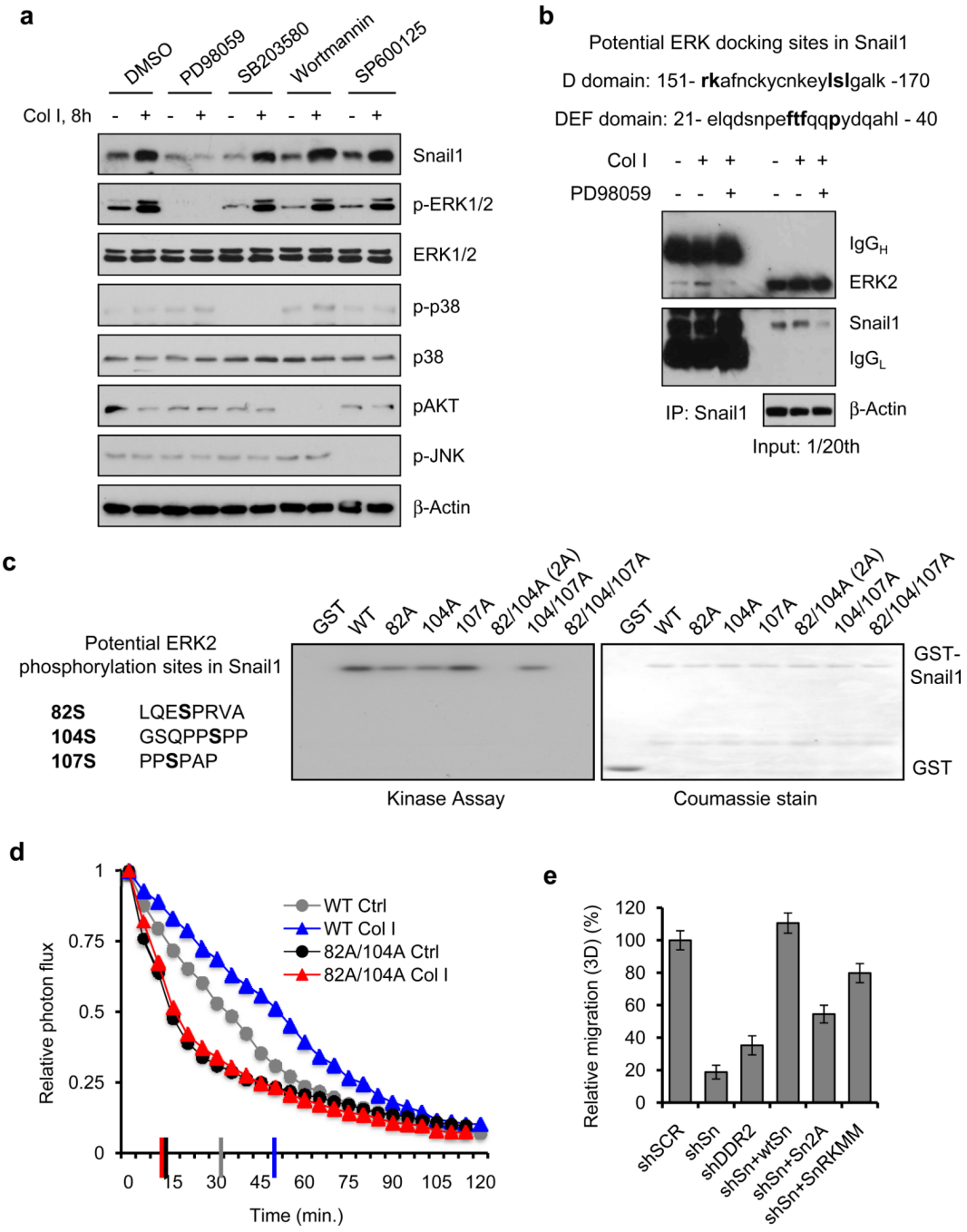

Figure 5. DDR2 stabilizes Snail1 protein through ERK2 phosphorylation of Snail1

(**a**) MDA-MB-231 cells added to collagen I coated (+) or uncoated plates (−) in the presence of inhibitors: DMSO; PD98059 (50 μM), MEKK1; SB203580 (20 μM), p38; Wortmannin (100 nM), PI3K; SP600125 (10 μM), JNK. Western blots were performed. (**b**) ERK D- or DEF-binding domains in human Snail1 (bold). MBA-MB-231 cells added to collagen I coated plates, +/− MEKK1 inhibitor PD98059, Snail1 immunoprecipitated and bound products Western blotted for the presence of ERK2 and Snail1. The right lanes are input controls. (**c**) In vitro kinase assays with purified ERK2 and GST-Snail1 or serine mutants (S–A) as substrate (2 μg).

Autoradiography (left), coumassie-stained gel of input proteins (right). (**d**) MDA-MB-231 cells containing WT Snail1-CBG or 82/104A.Snail1-CBG treated with cycloheximide (100 μg/ml), added to uncoated (Ctrl) or collagen I coated plates. Bioluminescence determined and plotted as photon flux relative to cell at t=0. The vertical Y-axis lines indicate half-life of each protein. (**e**) MDA-MB-231 cells depleted of Snail1 (shSn) or DDR2 (shDDR2) or control (shSCR) (columns 1–3). Snail1 depleted cells were rescued with RNAi-resistant WT Snail1, 2A – 82/104A Snail1 mutant, or the RK-MM – ERK D domain binding site Snail1 mutant. Cell migration in 3D collagen I gels relative to control cells was determined. Means and s.d. for three independent experiments; ten cell aggregates analyzed in each experiment. See Supplemental Figure S7a for experimental data.

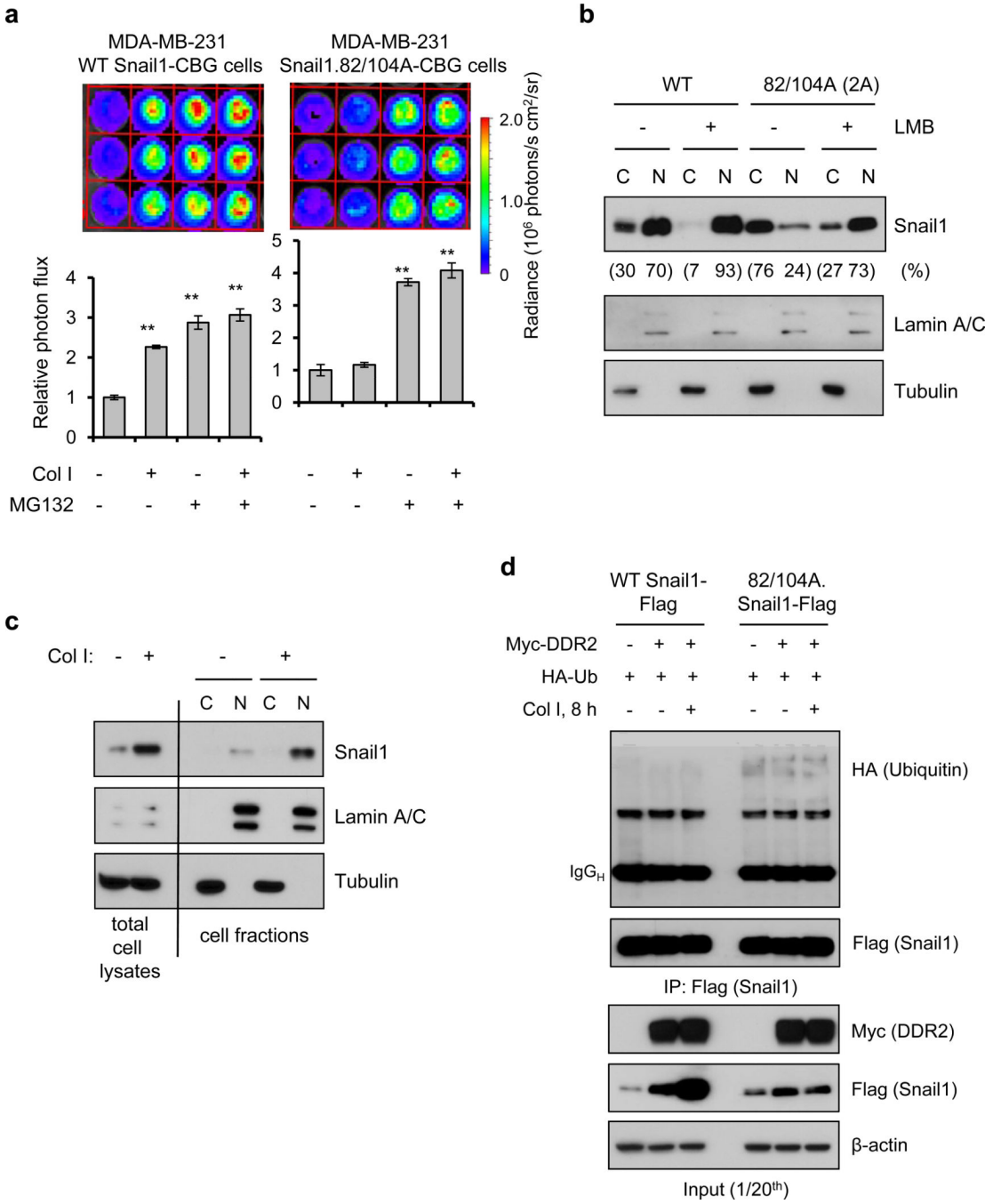

Figure 6. ERK2 phosphorylation of Snail1 results in nuclear accumulation and diminished ubiquitination

(**a**) MDA-MB-231 cells containing WT Snail1-CBG or 82/104A.Snail1-CBG were added to uncoated or collagen I coated wells for 8 hours +/− proteasome inhibitor MG132. Bioluminescence determined and results plotted relative to respective cells added to uncoated plates in the absence of MG132. Means and s.d. for three independent experiments; three wells of live cells analyzed each experiment. P-values calculated using unpaired, two-sided Student's t-tests. ** P<0.01. (**b**) MCF-10A cells transfected with WT Snail1 or 82/104A.Snail1 were treated with Leptomycin B (20 nM) (LMB) for 4 hours (+) or not (−). Cells lysed and nuclear (N) and cytosolic (C) fractions isolated. Western blots

were performed on subcellular fractions. The relative distribution of Snail1 between fractions was determined from densitometry. (**c**) MDA-MB-231 cells added to collagen I coated (+) or uncoated plates (−) for 8 hours. The first two lanes are Western blots of total cell lysates. Lanes 3–6 are Western blots of subcellular fractions: nucleus (N), cytosol (C). (**d**) HEK293 transfected with myc-DDR2, Snail1-Flag, and HA-Ubiquitin, as indicated. Cells were added to uncoated (−) or collagen I coated plates (+). No proteosome inhibitor was present. Snail1 was immunoprecipitated and bound products Western blotted (upper panels). Lower panels are input controls.

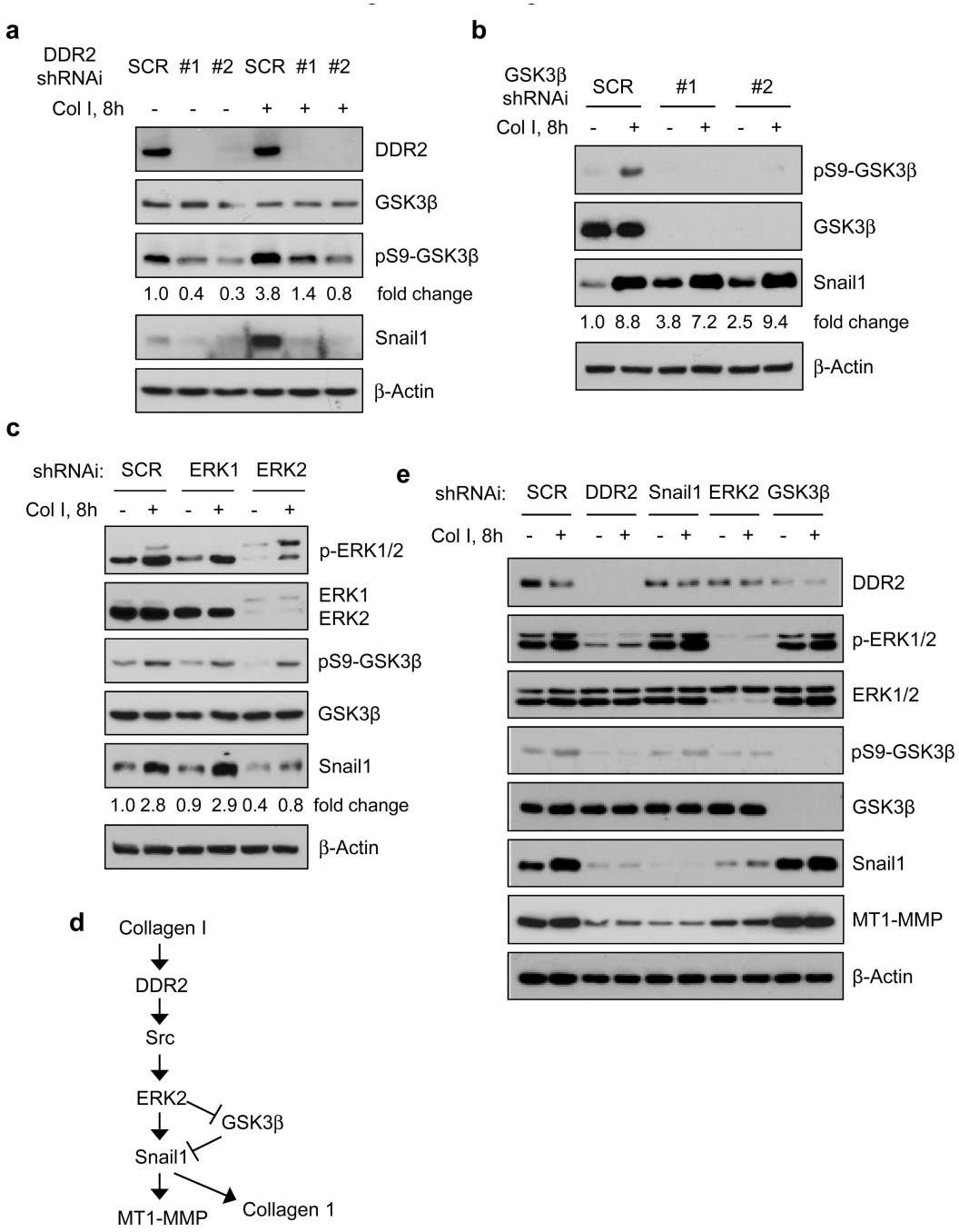

Figure 7. Delineation of the intracellular signaling pathway whereby DDR2 leads to Snail1 protein stabilization and tumor cell invasion/migration

(**a**) MDA-MB-231 cells shRNAi-depleted of DDR2 or control (SCR) were added to collagen I coated (+) or uncoated plates (−). Western blot with the indicated antibodies was performed on cell extracts. The fold change in phospho-S9-GSK3β relative to unstimulated control cells was calculated from densitometry. (**b**) MDA-MB-231 cells shRNAi-depleted of GSK3β or control (SCR) were added to collagen I coated (+) or uncoated plates (−). Western blots with the indicated antibodies were performed on cell extracts. The fold change in the level of Snail1 relative to unstimulated control cells was calculated from densitometry. (**c**) MDA-MB-231 cells shRNAi-depleted of ERK1 or ERK2 or control (SCR) were added to

collagen I coated (+) or uncoated plates (−). Western blots with the indicated antibodies were performed on cell extracts. The fold change in the level of Snail1 protein relative to unstimulated control cells was calculated from densitometry. (**d**) Proposed signaling pathway from collagen activated DDR2 to Snail1 stabilization and MT1-MMP and collagen I production. (**e**) MDA-MB-231 cells were shRNAi-depleted of the indicated proteins then added to collagen I coated (+) or uncoated plates (−). Cell extracts were Western blotted with the indicated antibodies.

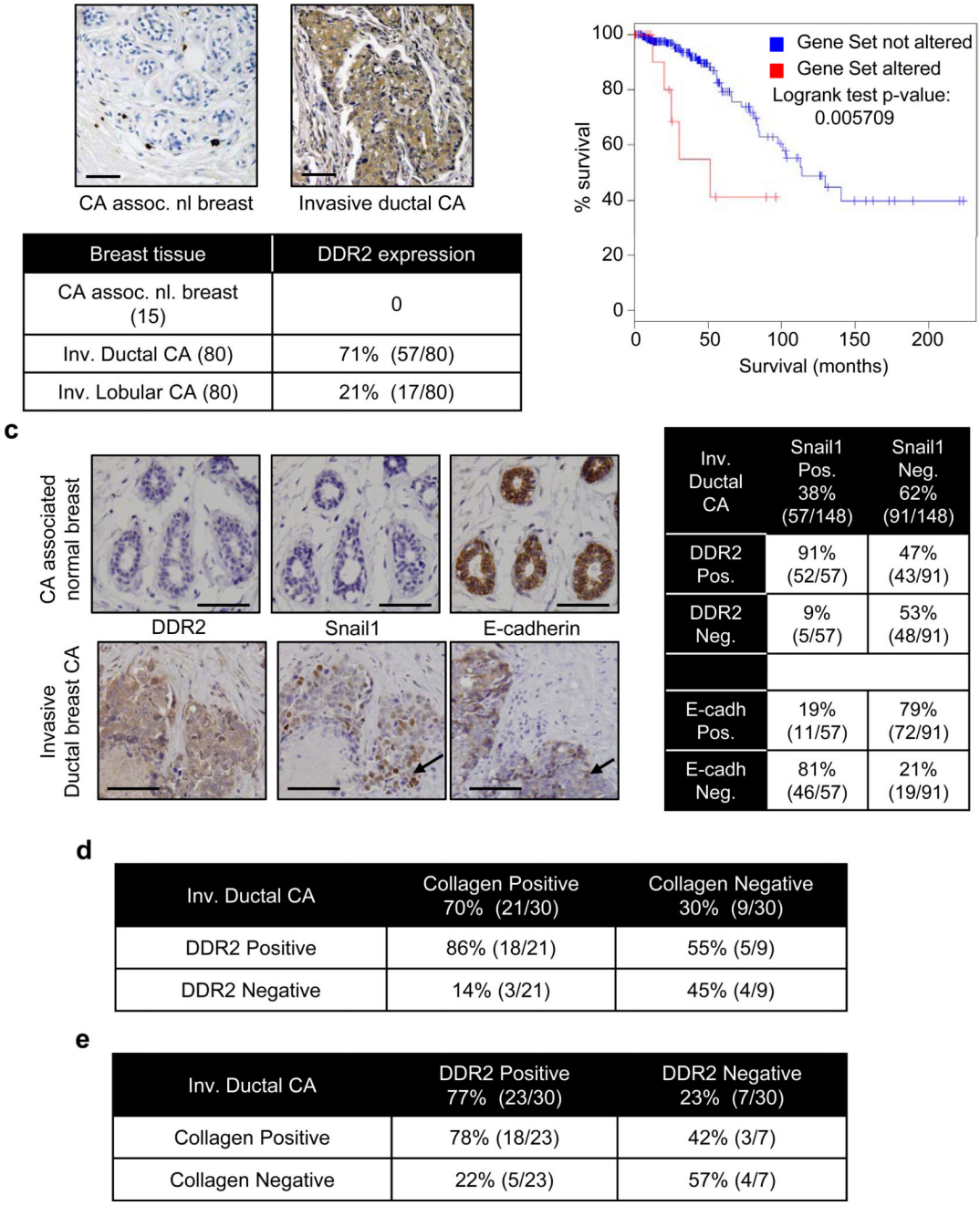

Breast tissue	DDR2 expression
CA assoc. nl. breast (15)	0
Inv. Ductal CA (80)	71% (57/80)
Inv. Lobular CA (80)	21% (17/80)

Inv. Ductal CA	Snail1 Pos. 38% (57/148)	Snail1 Neg. 62% (91/148)
DDR2 Pos.	91% (52/57)	47% (43/91)
DDR2 Neg.	9% (5/57)	53% (48/91)
E-cadh Pos.	19% (11/57)	79% (72/91)
E-cadh Neg.	81% (46/57)	21% (19/91)

d

Inv. Ductal CA	Collagen Positive 70% (21/30)	Collagen Negative 30% (9/30)
DDR2 Positive	86% (18/21)	55% (5/9)
DDR2 Negative	14% (3/21)	45% (4/9)

e

Inv. Ductal CA	DDR2 Positive 77% (23/30)	DDR2 Negative 23% (7/30)
Collagen Positive	78% (18/23)	42% (3/7)
Collagen Negative	22% (5/23)	57% (4/7)

Figure 8. DDR2 expression is present in the majority of human invasive ductal breast cancers and correlates with the presence of nuclear Snail1 and loss of E-cadherin expression

(**a**) Immunohistochemical analysis for DDR2 protein expression in 80 human invasive ductal carcinoma, 80 human invasive lobular carcinoma, or 15 cancer-associated normal breast samples. Shown is a representative example of invasive ductal carcinoma sample (right) and cancer-associated normal breast sample (left). Scale bar 100 μm. Results are tabulated in the table below. (**b**) Kaplan-Meier survival curve for 320 humans with invasive breast cancers. Gene copy number assessment at MSKCC cancer genome portal. 5% (18) have increased DDR2 gene copy number (red line). Blue line represents remaining patients with normal DDR2 gene copy number. (**c**) Immunohistochemical staining for DDR2, Snail1,

and E-cadherin in sequential slices of 148 invasive human ductal breast carcinoma or 20 cancer-associated normal breast samples. Shown is a representative sample of normal breast (upper panels) and invasive ductal carcinoma (lower panels). Black arrow indicates the presence of nuclear Snail1 staining in a DDR2 positive, E-cadherin negative sample. Scale bar equals 100 μm. Results are tabulated in the table of the right. (**d, e**) Immunohistochemical determination of DDR2 protein expression and collagen deposition (Trichrome stain) in 30 human invasive ductal carcinomas. (**d**) The percent of tumors with increased collagen deposition, or not, that expressed DDR2. (**e**) The percent of DDR2 positive or negative tumors that exhibited increased collagen deposition.